Fatigue Strength of Welded Joints under Multiaxial Loading in Terms of Local Strain Energy Density

F. Berto, P. Lazzarin

University of Padova, Department of Management and Engineering, Stradella San Nicola 3, 36100, Vicenza, Italy

ABSTRACT*. The approach based on the Strain Energy Density (SED) evaluated over a control volume is applied to summarise some fatigue strenght data of welded joints under multiaxial loading made of structural steel and aluminum alloys. The possible reasons of different slopes of the fatigue curves under multiaxial loading with respect to unixial loading have been discussed as well as some practical advantages tied to the use of coarse meshes in the SED evaluation.*

INTRODUCTION

The current approaches for the fatigue strength assessment of welded joints can mainly be divided into categories depending on the type of the stress analysis performed [1]. One can distinguish criteria based on nominal stress, structural stress, local stress or local strain as well as other approaches based on linear elastic Fracture Mechanics [2,3]. These approaches are separately summarised in the most recent Recommendations [4].
The main problems occurring in the application of local criteria are tied to the degree of arbitrariness in precisely defining the geometrical parameters [5]. The Effective Notch Stress method [6,7], suggests the introduction of a fictitious notch radius at the critical point of the structure. On the contrary, in the notch stress intensity approach [8-10], the concept of notch rounding is not applied and the weld toe is modelled as a sharp V-notch. Thus, the mode I and mode II Notch Stress Intensity Factors (NSIFs) can be used to quantify the magnitude of the asymptotic stress distribution [11]. In principle NSIFs are used to describe crack initiation at sharp notches [12, 13] just as stress intensity factors (SIFs) at crack-like notches. For its application the NSIF approach requires the knowledge of the elastic stress field in the region very close to the point of singularity. With this aim FE meshes must be very refined in the neighbourhood of the notch tip. The refinement required is far from easy to obtain in plane cases and very difficult and time expensive in three-dimensional cases. When the constancy of the weld toe angle is assured and the angle is large enough to make mode II contribution non-singular, the mode I N-SIF can directly be used to describe the fatigue strength of fillet welded joints having different geometries. The NSIFs are endowed with an odd dimensionality, which depends on the V-notch angle. Varying the angle, the comparability can be re-established by using the strain energy density averaged over a well-defined control

volume surrounding the weld root or the weld toe as a fatigue relevant parameter [14-18]. The radius R_0 of the averaging zone has been identified with reference to the conventional arc welding processes. For welded joints made of structural steels and aluminium alloys R_0 was found to be 0.28 mm and 0.12 mm, respectively.

The main aim of this contribution is to summarise the fundamentals of the method based on the averaged value of local strain energy density and to apply it to a large body of fatigue strength data reported in the literature [19-23] with reference to welded joints made of structural steel or aluminium alloy under multiaxial loading conditions. The scatterband has been drawn imposing at $2x10^6$ cycles the same value of local strain energy previously obtained from welded joints under traction or bending, but changing the slope (from 3/2 to 5/2 for steel weldments, from 4/2 to 6.5/2 dealing with aluminum alloys). It is confirmed the hypothesis that in high-cycle fatigue, where materials behaviour is generally thought as linear elastic, the critical value of strain energy density does not depend on the type of loading, being the same both under uniaxial and multiaxial fatigue. The inverse slope of the mean curve has been imposed.

The different role played by local and large scale yielding under tension and torsion loading is used to provide a possible explanation for the different slopes, 3.0 and 5.0, reported by Eurocode 3 and other Standards in force for welded details subjected to tensile or shear stresses, respectively. A very satisfactory agreement was found between the scatterband obtained by considering as main failure parameter the averaged SED and Ellyn's *fatigue master life curve* based on the use of the plastic strain energy per cycle as evaluated from the closed cyclic *hysteresis loop* and the positive part of the elastic strain energy density [24].

Moreover some important advantages of the mean value of the elastic SED as opposed to the direct evaluation of the NSIFs are highlighted in the paper. Among those advantages, the fact that the NSIF needs very refined meshes while on the contrary SED can be determined with high accuracy by using very coarse meshes [25, 26].

ANALYTICAL PRELIMINARIES

Local strain energy density $\Delta\overline{W}$ averaged in a finite size volume surrounding weld toes and roots is a scalar quantity which can be given as a function of mode I-II NSIFs in plane problems [14, 16] and mode I-II-III NSIFs in three dimensional problems [15, 17]. The evaluation of the local strain energy density needs precise information about the control volume size. From a theoretical point of view the material properties in the vicinity of the weld toes and the weld roots depend on a number of parameters as residual stresses and distortions, heterogeneous metallurgical micro-structures, weld thermal cycles, heat source characteristics, load histories and so on. To device a model capable of predicting R_0 and fatigue life of welded components on the basis of all these parameters is really a task too complex. Thus, the spirit of the approach is to give a simplified method able to summarise the fatigue life of components only on the basis of geometrical information, treating all the other effects only in statistical terms, with reference to a well-defined group of welded materials and, for the time being, to arc welding processes.

In a plane problem all stress and strain components in the highly stressed region are correlated to mode I and mode II NSIFs. Under a plane strain hypothesis, the strain energy included in a semicircular sector shown in Figure 2 is [14, 17]

$$\Delta\overline{W} = c_w \left\{ \frac{e_1}{E}\left[\frac{\Delta K_1^N}{R_C^{\,1-\lambda_1}}\right]^2 + \frac{e_2}{E}\left[\frac{\Delta K_2^N}{R_C^{\,1-\lambda_2}}\right]^2 + \frac{e_3}{E}\left[\frac{\Delta K_3^N}{R_C^{\,1-\lambda_3}}\right]^2 \right\} \quad (1)$$

where R_0 is the radius of the semicircular sector and e_1, e_2 and e_3 are functions that depend on the opening angle 2α and the Poisson ratio ν [17].

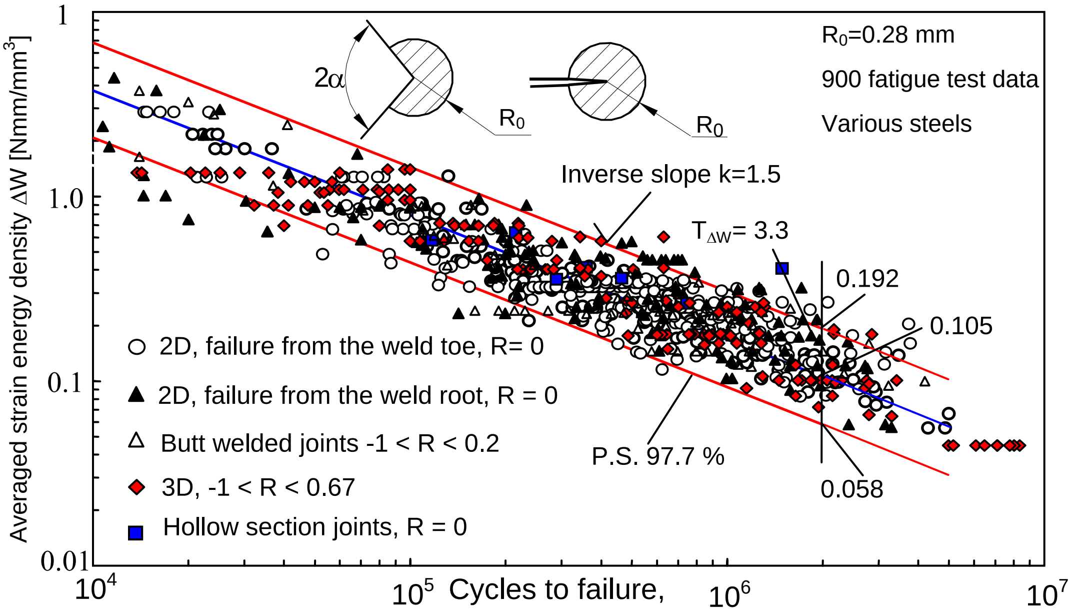

Fig. 1. Fatigue strength of welded joints as a function of the averaged local strain energy density; R is the nominal load ratio [18]

In Eq.(2) the coefficient c_W allows us to take into account the influence of the nominal load ratio R in the case of post-welding treatments (stress-relieved joints). In particular, according to the expressions for c_W given in Ref. [15], we shall use here c_W=1 for R=0 and c_W=0.5 for R=-1. For all welded joints under as-welded conditions one should assume c_W=1, independently of R.

The material parameter R_0 can be estimated by using the fatigue strength $\Delta\sigma_A$ of the butt ground welded joints (in order to quantify the influence of the welding process, in the absence of any stress concentration effect) and the NSIF-based fatigue strength of welded joints having a V-notch angle at the weld toe constant and large enough to ensure the non singularity of mode II stress distributions.

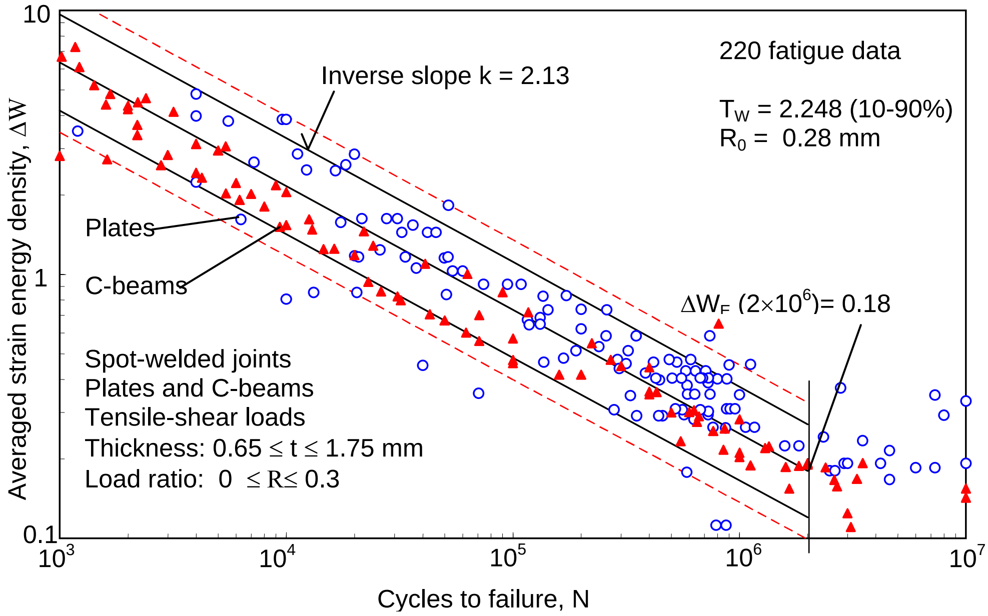

Fig. 2. Synthesis of data from spot-welded joints under tension and shear loading. The thickness t ranges from 0.65 to 1.75 mm [18].

A convenient expression is [14]:

$$R_0 = \left(\frac{\sqrt{2e_1}\ \Delta K_{1A}^{N}}{\Delta \sigma_A} \right)^{\frac{1}{1-\lambda_1}} \qquad (2)$$

where both λ_1 and e_1 depend on the V-notch angle. Eq. (3) makes it possible to estimate the R_0 value as soon as ΔK_{1A}^{N} and $\Delta\sigma_A$ are known. F For welded joints made of structural steels and aluminium alloys R_0 was found to be 0.28 mm and 0.12 mm, respectively. By modelling the weld toe regions as sharp V-notches and using the local strain energy, Livieri and Lazzarin summarised more than 600 fatigue strength data from welded joints with weld root and toe failures and obtained the theoretical scatter band in terms of SED [16]. The geometry exhibited a strong variability of the main plate thickness (from 6 to 100 mm), the transverse plate (from 3 to 200 mm) and the bead flank (from 110 to 150 degrees). A final synthesis based on 900 experimental data is shown in Figure 1 where some recent results from butt welded joints, three-dimensional models and hollow section joints have been included. A good agreement is found, giving a sound, robust basis to the approach when the welded plate thickness is equal to or greater than 6 mm [18]. A first synthesis of data from single spot-welded joints characterized by thin plates (0.65 mm≤t≤1.75 mm) is shown in Figure 2. The control radius of the three-dimensional volume around the slit tip and its depth are equal to 0.28 mm. The value of $\Delta\overline{W}$ at 2x10^6 cycles is higher than that reported in Figure 1.

SOME ADVANTAGES OF THE SED

As opposed to the direct evaluation of the NSIFs, which needs very refined meshes, the mean value of the elastic SED on the control volume can be determined with high accuracy by using coarse meshes [25-26]. Very refined meshes are necessary to directly determined the NSIFs from the local stress distributions. Refined meshes are not necessary when the aim of the finite element analysis is to determine the mean value of the local strain energy density on a control volume surrounding the points of stress singularity. The SED in fact can be derived directly from nodal displacements, so that also coarse meshes are able to give sufficiently accurate values for it. Some recent contributions document the weak variability of the SED as determined from very refined meshes and coarse meshes, considering some typical welded joint geometries and provide a theoretical justification to the weak dependence exhibited by the mean value of the local SED when evaluated over a control volume centred at the weld root or the weld toe. On the contrary singular stress distributions are strongly mesh dependent.
The typical coarse mesh used to evaluate the SED at the weld toe or root consists of eight elements in the control volume and about forty elements in the entire model being negligible the difference in terms of SED with the results obtained from finer meshes used for the NSIFs evaluation.
The different role played by local and large scale yielding under tension and torsion loading provided an interesting interpretation for the different slopes, 3.0 and 5.0, reported by Eurocode 3 and other Standards in force for welded details subjected to tensile or shear stresses, respectively [34].

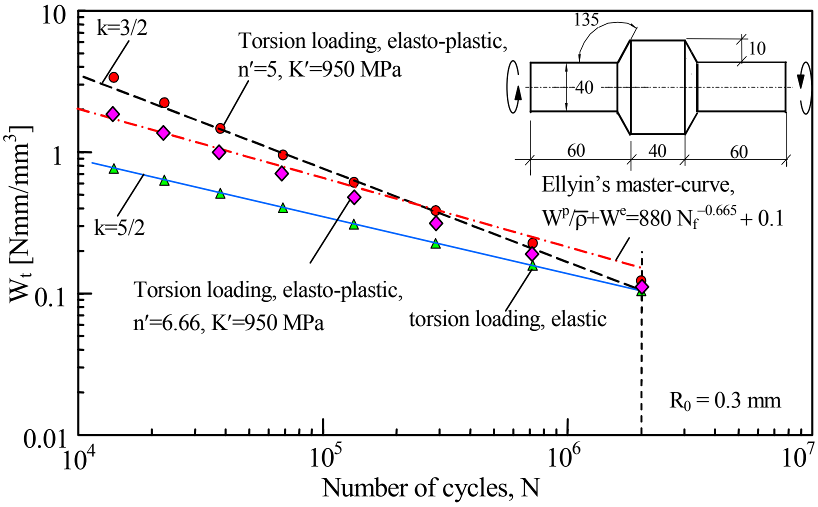

Figure 3. Total SED under linear elastic and elastic-plastic conditions

A very satisfactory agreement was found between the scatterband obtained by considering as main failure parameter the averaged SED and Ellyn's *fatigue master life curve* based on the use of the plastic strain energy per cycle $\Delta\tilde{W}^P$ as evaluated from the closed cyclic *hysteresis loop* and the positive part of the elastic strain energy density $\Delta\widetilde{W}^{e+}$.

MULTIAXIAL FATIGUE LOADING OF WELDED JOINTS

Fatigue strength data of welded joints made of structural steels have been re-analysed in terms of local energy. For each geometry considered herein, original papers reported different series of experimental data [19-21].

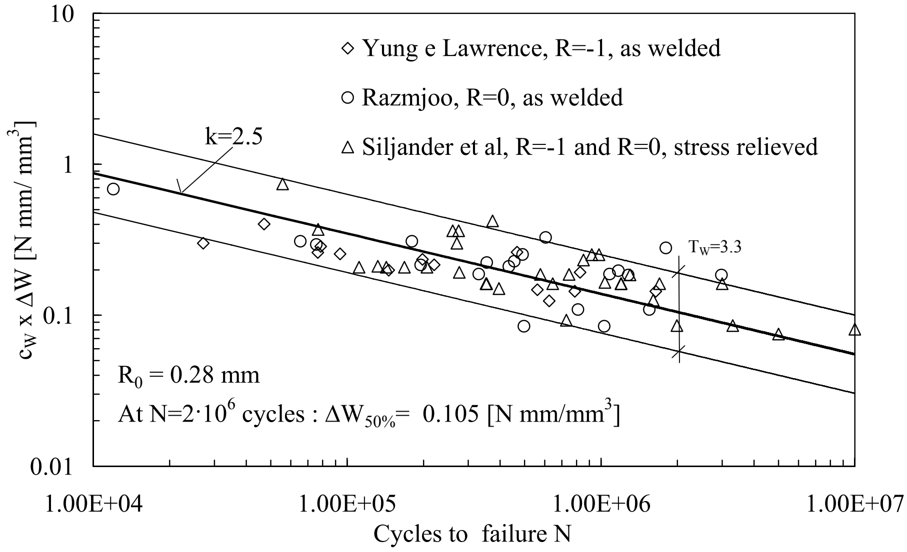

Figure 4. Synthesis of data from welded joints under multiaxial loading in terms of local energy

Fig. 4 summarises all the data in terms of the mean value of the strain energy density and present a comparison with a multiaxial scatterband. The scatterband has been drawn imposing at $2x10^6$ cycles the same value of local strain energy previously obtained from welded joints under traction or bending, but changing the slope (from 3/2 to 5/2). It is confirmed the hypothesis that in high-cycle fatigue, where materials behaviour is generally thought as linear elastic, the critical value of strain energy density does not depend on the type of loading, being the same both under uniaxial and multiaxial fatigue. The inverse slope of the mean curve has been imposed equal to 2.5, according to Ref. [15]. When reconverted in terms of local stress, instead of local energy, it coincides with the value k=5 suggested by Eurocode 3 for a generic "shear load", in the absence of a clear distinction between stress components due to shear or torsion loading. The comparison between experimental data, in terms of local energy, and the scatterband proposed is satisfactory and shows how all data are well distributed around the mean curve with the exception of some data due to Razmjoo, which seem to be affected by a larger scatter. In particular 3 data obtained under pure torsion and R=0 are slightly higher than expected whilst, on the contrary, some values are a little lower under pure traction and the same load ratio, R=0. All results have been obtained from linear elastic FE analyses.

Fatigue strength data of welded joints made of aluminium alloys have been also re-analysed. Different series of experimental data were taken from the literature [22, 23]. Figure 5 summarises all fatigue strength data in terms of the mean value of the strain energy density also comparing them with a multiaxial scatterband for aluminium alloys. The proposed curve has been drawn imposing at $2x10^6$ cycles the same value of local energy already obtained in references [16] summarizing a large amount of experimental data referred to welded joints made of aluminium under traction or bending. The inverse slope of the mean curve has been imposed equal to 3.25, following the precise suggestion reported in ref. [15], where the slope of the stress-based band was 6.5. The comparison between the experimental data reconverted in terms of local energy and the scatterband proposed is satisfactory.

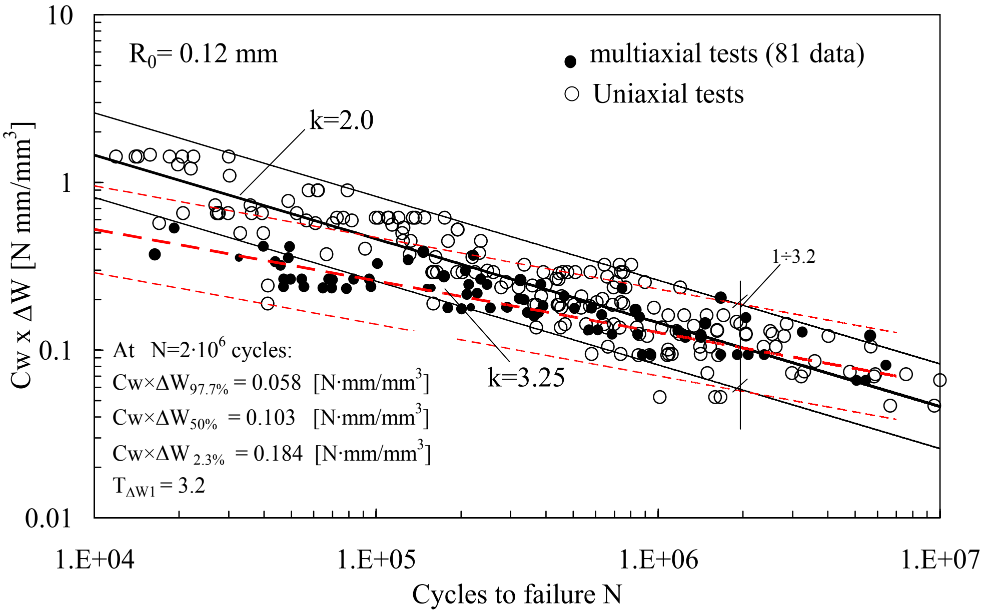

Figure 5. Synthesis of data from welded joints under multiaxial loading in terms of local energy. A comparison with data from uniaxial tests is carried out.

CONCLUSIONS

A re-analysis of data taken from the literature and dealing with steel and aluminum welded joints under multiaxial loading is carried out in the present paper. At two million cycles, the mean value of the strain energy density has found to be in agreement with the value obtained from tensile and bending loading. The different slopes of the scatterband under multiaxial loading, observed both for steel and aluminum weldments, is in agreement with those reported in the literature (and in some Standards in force). A motivation of a different slope under uniaxial or multiaxial fatigue cannot be provided on the basis of linear elastic hypothesis and a possible explanation should involve the different influence that tensile and torsion loads have on the local yielding in the highly stressed regions.

References

1. Radaj, D., Sonsino, C.M., Fricke, W. (2006) *Fatigue assessment of welded joints by local approaches*, Woodhead Publishing, Cambridge.
2. Maddox, S.J. (1987). *The Effect of Plate Thickness on the Fatigue Strength of Fillet Welded Joints*. Abington Publishing, Abington, Cambridge.
3. Gurney, TR. (1991). *The fatigue strength of transverse fillet welded joints*. Abington Publishing, Cambridge.
4. Hobbacher, A. (Ed.). (2005) *Fatigue design of welded joints and components*, Abington Publishing, Cambridge 2005 (updated edn.).
5. Radaj, D. (1996) *Int J Fatigue* **18**, 153-170.
6. Radaj, D. (1969) Näherungsweise Berechnung der Formzahl von Schweiβnähten. *Schw. Schn.* **21**(3): 97-105, and **21**(4):151-158.
7. Radaj, D. (1990) *Design and analysis of fatigue resistant welded structures*, Abington Publishing, Cambridge.
8. Lazzarin, P. Tovo R. (1998) *Fatigue Fract Eng Mater Struct* **21**, 1089-1104.
9. Tovo, R., Lazzarin, P. (1999) *Int J Fatigue* **21**, 1063-1078.
10. Lazzarin, P., Livieri, P. (2001) *Int J Fatigue* **23**, 225-232.
11. Williams, ML. (1952) *J Applied Mech* **19**, 526-528.
12. Boukharouba, T, Tamine, T, Nui, L, Chehimi, C, Pluvinage, G. (1995) *Engng Fract Mech* **52**, 503-512.
13. Verreman, Y, Nie, B. (1996) *Fatigue Fract Eng Mater Struct* **19**, 669-681.
14. Lazzarin, P., Zambardi, R. (2001) *Int J Fract* **112**, 275-298.
15. Lazzarin, P., Sonsino, C.M., Zambardi R. (2004) *Fatigue Fract Engng Mater Struct* **27**, 127-141.
16. Livieri, P., Lazzarin, P. *Int J Fract* 2005 **133,** 247-276.
17. Lazzarin, P., Livieri, P., Berto, F., Zappalorto, M. (2008), *Engng Fract Mech* **75**, 1875-1889.
18. Berto, F., Lazzarin, P. (2009) *Theor Appl Fract Mech* **52,** 183-194.
19. Yung, JY, Lawrence, FV. Predicting the Fatigue Life of Welds Under Combined Bending and Torsion. Report No. 125, UIL-ENG 86-3602, 1986, University of Illinois at Urbana-Champaign.
20. Siljander, A, Kurath, P, Lawrence, FV. (1992) Non-proportional fatigue of welded structures. In: Advances in Fatigue Lifetime Predictive Techniques. ASTM STP 1122 Philadelphia; ASTM, PA, 319–338.
21. Razmjoo, GR. (1996) Fatigue of Load-Carrying Fillet Welded Joints Under Multiaxial Loadings. TWI, Cambridge, UK: Abington (TWI REF. 7309.02/96/909).
22. Kueppers M, Sonsino CM. (2003) *Fatigue Fract Engng Mater Struct* **26**, 507-513.
23. Costa, JDM, Abreu, LMP, Pinho, ACM, Ferreira, JAM. (2005) *Fatigue Fract Engng Mater Struct* **28**, 399–407.
24. Ellyin, F. (1997), *Fatigue Damage, Crack Growth and Life Prediction*, Chapman & Hall, London.
25. Lazzarin, P., Berto, F., Gomez, FJ., Zappalorto, M. (2008). *Int J Fatigue* **30**, 1345-1357.
26. Lazzarin, P., Berto, F. (2008) *Fatigue Fract Eng Mater Struct* **31**, 95-107.